A Super-resolution Locationing Algorithm for Ultra-wideband phased-array radars

Toru SATO and Seiji HORITA
Department of Communications and Computer Engineering, Kyoto University
Kyoto, 606-8501, Japan

Abstract— **Super-resolution direction finding algorithms such as MUSIC or ESPRIT methods inherently assume narrow-band signals, which are not applicable to ultra-wideband radars such as GPR (ground penetration radar). We developed a time-domain algorithm to determine the time and direction of arrival pulses with an order higher resolutions than the nominal resolution determined by the aperture size. The received signal waveform at each array element is first analyzed by the recursive non-orthogonal decomposition using a dictionary of basic waveforms. After the delay time of the echoes in each element of the receiving array is determined, the number of targets and their locations are determined by analyzing variation of the delay time over the array with the aid of Hough transform. The robustness of the proposed algorithm is confirmed by numerical simulations.**

Keywords—**Super-resolution, recursive non-orthogonal decomposition, ground penetrating radar, radar imaging, direction finding.**

I. Introduction

GROUND penetration radars (GPR) often suffer from their poor resolution. Because of the increasing attenuation with frequency, the effective aperture size is usually limited to several wavelengths, which limits the angular resolution. Range resolution is also restricted by the wavelength. It is common to use baseband pulses in order to achieve the highest range resolution at the given frequency band, which is determined by the required penetration depth.

Here we present a solution to this problem by developing a super-resolution technique applicable to GPR's. Existing super-resolution direction finding algorithms such as MUSIC[1] or ESPRIT methods inherently assume narrow-band signals, which are not applicable to ultra-wideband radars. We have developed imaging algorithms for GPR based on the model fitting[2], which requires a good initial guess of the location of targets. Our objective is to develop a non-parametric super-resolution direction finding algorithm aimed for such applications.

II. Analysis of Waveforms

A. Extension of MUSIC Principle for Ultra-wideband Signals

We assume a radar system with a transmit/receive array and multiple targets in its near field. The basic approach is to decompose the received signal into Fourier components, apply MUSIC to each of them, and synthesize the results. The MUSIC spectra of all frequencies are summarized to give

$$P_{\mathrm{MU_{all}}}(\theta) = \frac{1}{\dfrac{1}{P_{\mathrm{MU_1}}(\theta)} + \dfrac{1}{P_{\mathrm{MU_2}}(\theta)} + \cdots \dfrac{1}{P_{\mathrm{MU}_L}(\theta)}} \ , \quad (1)$$

which should be maximized.

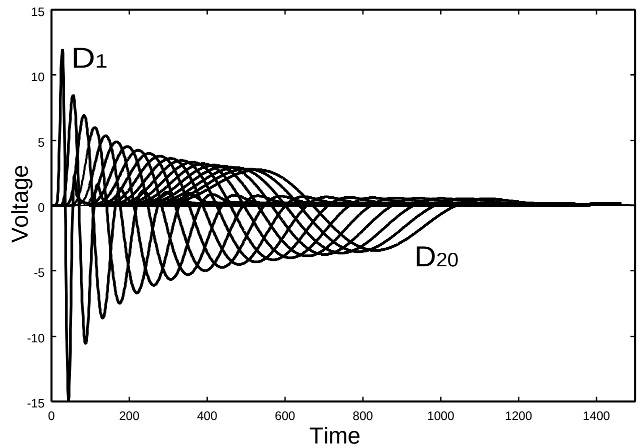

Fig. 1. Dictionary waveforms used for recursive non-orthogonal decomposition.

B. Decomposition with Dictionary Waveforms

Major problem with this approach is that ordinary criteria for the number of arrival waves, such as AIC, cannot be used, because sinusoids at each band are totally coherent with each other. We thus employ a time-domain approach in determining the number of arrival waves.

We first detect target echoes from time series of the receiver output of each array element. The received waveform is decomposed by the recursive non-orthogonal decomposition[3], [4] with dictionary waveforms. The input signal $f(t)$ is expressed in terms of dictionary waveforms $g_{\gamma n}(t)$ as

$$f(t) = \sum_{n=0}^{m-1} \{C^n \cdot g_{\gamma n}(t)\} + R^m f(t) \ , \quad (2)$$

where $R^m f(t)$ is the residual at m's iteration. The coefficient C^n is the cross correlation between $f(t)$ and the best fit $g_{\gamma n}(t)$, which is determined by maximizing

$$C^n = \int_{-\infty}^{\infty} R^{n-1} f(t) \cdot g_{\gamma n}(t) \mathrm{d}t \ . \quad (3)$$

Fig. 1 shows examples of the dictionary waveforms used in the present paper. Here we select a mono-cycle pulse waveform as the 'mother wavelet,' and stretch it assuming the constant-Q propagation model[5] in the subsurface environment. It is known that the attenuation coefficient of the subsurface medium is roughly proportional to the frequency. Under such condition, a wave packet loses its higher frequency

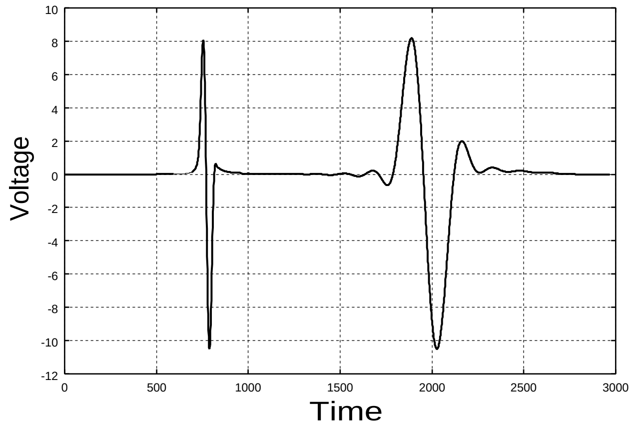

Fig. 2. Simulated waveform for recursive decomposition.

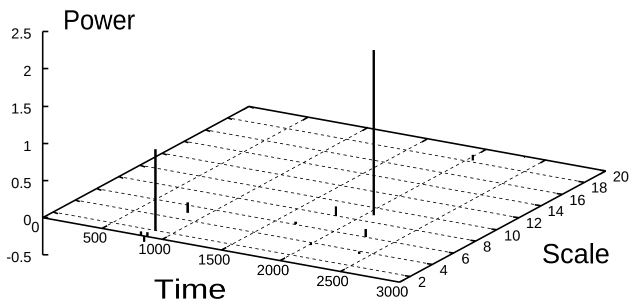

Fig. 3. Result of the non-orthogonal recursive decomposition.

components as it propagates in a manner that its envelope and the carrier frequency stretches simultaneously, conserving the Q-factor of the wave packet.

Iterations are repeated until the residual waveform satisfies the whiteness condition. Since the amplitude of the random Gaussian noise follows Rayleigh distribution, existence of other signals can be detected by fitting the shape of the cumulative distribution function of residual function $R^m f(t)$ with that of the Rayleigh distribution. The shape of the distribution is determined from the lowest 1/3 of its cumulative distribution, and its deviation due to remaining signal components is measured using the rest of the distribution. When the received signal is dominated by clutters as is often the cases for GPR signals, the Weibull distribution is used in place of the Rayleigh distribution, although the sensitivity of detection slightly deteriorates.

Fig. 2 is an example of simulated waveform for the case of two point targets embedded at different depth. The waveform of the deeper target has a narrower bandwidth due to the longer travel time through the medium, and the increasing attenuation with increasing frequency. No noise is added in this example. Fig. 3 shows the power of decomposed waves in terms of their time and scale. The scale numbers are the same as those attached to the waveforms in Fig. 1.

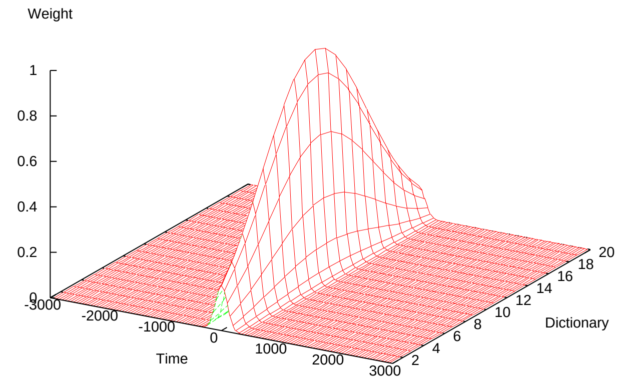

Fig. 4. The weighting function used to unify neighboring points in time–scale space.

C. Identification of Wave Packets

When the received echo from a target has a deformed waveform, it is represented by a combination of multiple dictionary waveforms as shown by the small components around the two major peaks in Fig. 3. They are unified by a variant of the collapsing algorithm[6], which moves each point to the center of the gravity of its surrounding points. A point with a position vector $\boldsymbol{p}_{0i}$ in the time–scale space is moved to a new position

$$\boldsymbol{p}_{1i} = \sum_{\boldsymbol{p}_{0j} \in N(\boldsymbol{p}_{0i})} w(\boldsymbol{p}_{0j} - \boldsymbol{p}_{0i}) \boldsymbol{p}_{0j} / M(\boldsymbol{p}_{0i}) \; , \qquad (4)$$

where $N(\boldsymbol{p})$ is a neighbor space around point $\boldsymbol{p}$, $w(\boldsymbol{p})$ is a Gaussian weighting function as shown in Fig. 4, and $M(\boldsymbol{p})$ is the number of points in $N(\boldsymbol{p})$. A narrow window is used for the time axis in order to select only those components appearing simultaneously, while a wide window is used for the scale axis to absorb higher harmonics. The procedure is repeated until stable grouping is obtained. Decomposed components shown in Fig. 3 are successfully unified into the two desired components by this procedure. Received signals of unknown waveforms can thus be identified as a group of wave packets as far as their waveforms have some similarity to those of the dictionary waveforms.

III. Determination of Target Location

After the delay time of the echoes at each element of the receiving array is determined, the number of targets and their locations are determined by analyzing variation of the delay time over the array. Fig. 5 plots the delay time multiplied by the velocity of the waves versus the distance of the array elements from its origin applied for a set of simulated data. Three pulses are assumed to arrive from -60, -20, and 45 degrees from the baseline of the array. The waveforms of the first two pulses are the same as shown in Fig. 2, and the third pulse has the

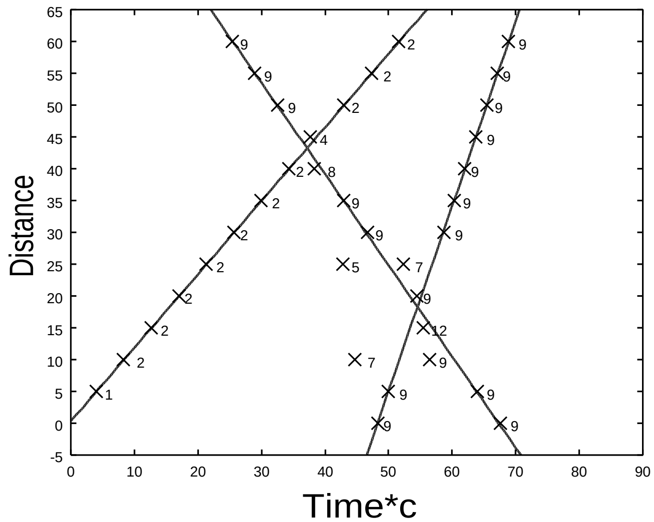

Fig. 5. Detected points and estimated traces of targets on a delay-distance plane.

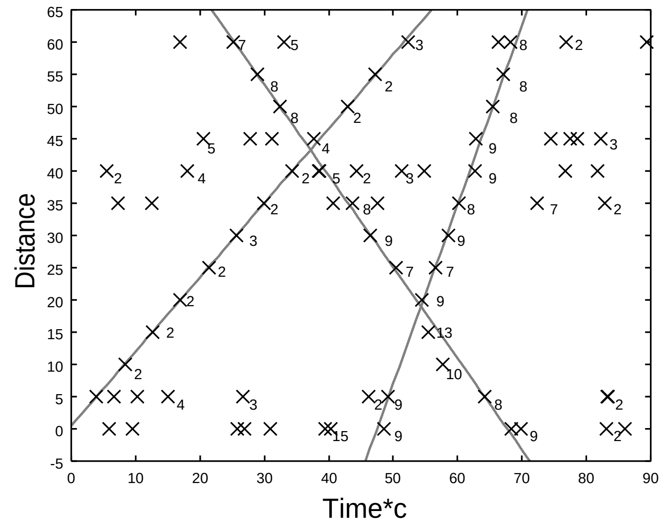

Fig. 6. Same as Fig. 5, but for S/N=12dB.

same shape as the second one, simulating the condition of multipath reflections. Each symbol denotes a detected signal by the above analysis, and the attached numbers indicate the dictionary waveforms.

As the echoes from a single target conform a straight line in this plot, the number and the location of targets can be precisely determined by fitting lines on it. A straight line in $x-y$ plane is expressed in terms of its distance ρ from the origin and the inclination angle θ as

$$\rho = x\cos\theta + y\sin\theta \;, \tag{5}$$

which gives the Hough transform. Since all points on a line in (x, y) space is transformed into a point (ρ, θ), straight lines are detected by choosing points with high concentration in the (ρ, θ) space. Straight lines in Fig. 5 are obtained by applying Hough transform to these points. The result clearly identifies three targets. Although the analyses of individual waveforms of each array element sometimes make wrong selection especially when multiple echoes appear at the same delay, they are recovered by the line detection process.

Error analyses of the obtained results by numerical simulations showed that the proposed method has about 10–20 times higher angular accuracies than that of ordinary phased arrays. An advantage of this method is that this resolution does not deteriorate even for the cases with noises. Fig. 6 is same as Fig. 5, but for the signal-to-noise of 12dB. Although more erroneous points are detected in the step of waveform analysis of each array element, they are removed by the line detection process, and the accuracy of the estimated angle of arrival stays almost unchanged.

The separation of multiple pulses are naturally better when they have different scales as shown by the left two lines of Fig. 5, while a larger disturbances appear at around the intersection of the right two lines which have the same waveform. A further study is needed to quantitatively examine the performance of the proposed algorithms in realistic conditions. It should be noted that although the current study is limited to two-dimensional cases, extension to the three-dimensional case is simple and straightforward.

IV. Summary

A robust and high-resolution scheme has been developed for determining the time and direction of arrival pulses with various waveforms. Received signals at each array element are analyzed by decomposing with dictionary waveforms, and successfully identified even when it is deformed due to propagation characteristics of the medium. The direction of arrival is then determined from times of arrival at each element with the aid of Hough transform, which detect straight lines from points distributed in the time-distance plane.

References

[1] R. O. Schmidt, “Multiple emitter location and signal parameter estimation,” *IEEE Trans. Antennas Propagat.*, Vol. 34, No. 3, pp. 276–280, 1986.

[2] T. Sato, T. Wakayama, and K. Takemura, “An imaging algorithm of objects embedded in a lossy dispersive medium for subsurface radar data processing,” *IEEE Trans. Geosci. Remote Sens.*, Vol. 38, No. 1, pp. 296–303, 2000.

[3] S. G. Mallat and Z. Zhang, “Matching pursuits with time-frequency dictionaries,” *IEEE Trans. Signal Processing*, Vol. 41, No. 12, pp. 3397–3415, 1993.

[4] T. Sato and Y. Tada, “Noise reduction and identification of subsurface radar images using recursive wavelet decomposition,” *Proc. 2000 IEEE Int. Geosci. Remote Sens. Symp.*, pp. 660–662, 2000.

[5] G. Turner, “Propagation deconvolution,’ *Proc. 4th Int. Conf. Ground Penetrating Radar*, pp.85–93, 1992.

[6] R. H. Jones, “A method for determining significant structures in a cloud of earthquakes,” *J. Geophys. Res.*, Vol. 102, No. B4, pp. 8245–8254, 1997.